ELSEVIER

Journal of Alloys and Compounds 217 (1995) 112–117

Journal of ALLOYS AND COMPOUNDS

Stability of the hydrogen absorption and desorption plateaux in $LaNi_5$–H
Part 3: experimental observations of compositional inhomogeneities due to temperature gradients

E.H. Kisi[a], E. MacA. Gray[b,*]

[a]*Department of Mechanical Engineering, University of Newcastle, Newcastle, NSW 2308, Australia*
[b]*School of Science, Griffith University, Brisbane, Qld. 4111, Australia*

Received 31 May 1994

Abstract

It has been predicted by Pons and Dantzer that temperature gradients due to the released enthalpy of H absorption–desorption will generate macroscopic inhomogeneities of the α/β phase proportions in metal hydrides. We used in situ X-ray diffraction and in situ neutron diffraction respectively to study the growth of β-$LaNi_5$–H at the free surface, and β-$LaNi_5$–D in the bulk of powdered samples. It was found that a macroscopic compositional inhomogeneity does occur, and can be so severe that the free surface of the sample remains pure α phase while the bulk of the sample is rich in β phase.

Keywords: Stability; Hydrogen absorption; Hydrogen desorption; Metal hydrides

1. Introduction

Experiments on metal hydrides are almost universally predicated on the (usually implicit) assumption that the phase proportions of the sample do not vary throughout its volume. It has recently been reported [1] that this assumption is unwarranted in most cases. This conclusion arose from an experiment conducted in an isochoral (i.e. constant volume) hydrogenator, in which $LaNi_5$–H was heated by about 25 °C, starting from a hydrogen content on the absorption plateau. After cooling back to the initial temperature, the static H_2 pressure had dropped by about 20 kPa from its initial value of 200 kPa.

This result was explained as a consequence of a compositional inhomogeneity developing in the powdered hydride due to thermal gradients, as follows. In any but the thinnest samples, the temperature of some sample fraction (designated B) is less constant than that of a fraction (designated A) adjacent to the heat sink/source, because of the higher intervening thermal resistance due to the longer path for heat flow. During an upward temperature pulse applied at the heat sink, A desorbs quickly and raises the system pressure, causing B to absorb. As the hydride cools, A reabsorbs and B desorbs. The end result is that both fractions are in the region between the absorption and desorption plateaux with significantly different local proportions of the α and β phases. A thermal model was developed and solved numerically, giving good agreement with the above experimental results [1].

The consequences of compositional inhomogeneities are widespread. Two of the most important affect the experimental characterization of hydrides, and thereby both microscopic and macroscopic models of their behaviour. First, as discussed in the preceding paper in this series [2], compositional inhomogeneities are expected also to cause false measurements of plateau pressures. This is believed to be the origin of the so-called large-aliquot effect in its various guises and is treated at length in [2]. Second, techniques which are sensitive to the relative proportions of the α and β phases will give different answers from different volume fractions of the sample. This effect is potentially very severe in in situ X-ray diffraction studies, where the incident beam typically penetrates the sample to only a few micrometres. Thus data obtained under particular conditions of steady pressure and uniform steady temperature might be quite unrepresentative of the sample as a whole, owing to its detailed thermal history. Even

*Corresponding author.

SSDI 0925-8388(94)01311-5

using neutron diffraction, which samples the whole volume of material, the results will be an average over an unknown spatial distribution of local α/β phase proportions ranging in principle from pure α to pure β.

This paper is concerned with demonstrating experimentally that severe compositional inhomogeneities do indeed occur owing to temperature gradients. We report measurements by both X-ray and neutron powder diffraction (XRD, ND) on $LaNi_5$ hydrides and deuterides respectively using in situ techniques.

2. Experimental details

Samples of $LaNi_5$ powder (Research Chemicals alloy #1241, $LaNi_{4.93}$) were prepared by mechanical grinding followed by at least five complete cycles of H or D absorption and desorption as appropriate to the diffraction technique. The same hydrogenator was used for both XRD and ND, with different sample cells. Ultrahigh purity H_2 was used for XRD, but for ND D_2 is necessary because of the high incoherent neutron scattering cross-section of H. The D_2 was stored as $LaNi_5$–D in a separate reservoir and supplied or recovered by adjusting the temperature of the storage bed. H or D absorption by the metal was measured by filling a known reference volume to a selected pressure, opening this volume to the sample space, and observing the pressure decrease in the total volume so formed. A resolution in the hydrogen-to-metal ratio [H]/[M] of about 0.02 (XRD) and 0.01 (ND) was achieved, depending mainly on the volumes of the sample and reference chambers relative to the equivalent H_2 capacity of the sample. The pressure in the sample cell, the sample temperature and diffraction patterns were recorded at time intervals ranging from a few minutes to many hours after the gas pressure was raised or lowered to absorb or desorb H or D.

The basis for discrimination of the α and β phases is the 24% volume expansion accompanying the α–β transformation. Distinct diffraction patterns are readily measured for the two phases, whose proportions we determined quantitatively by Rietveld profile analysis, according to a procedure described elsewhere [3].

2.1. X-ray diffraction

The diffractometer (Philips PW1820 with proportional counter) is fitted with a sample chamber able to withstand 1 MPa of H_2 and was operated in Bragg–Brentano reflection geometry with Co Kα radiation and Fe diffracted-beam filter. The temperature of the sample was measured by a thermocouple buried within the powder, 0.5 mm below its surface and closely adjacent to the footprint of the X-ray beam. The sample holder, shown in Fig. 1, is heated from below. Large samples are necessary so that the average [H]/[M] atomic ratio can be calculated accurately from the pressure change during absorption or desorption of an aliquot of H_2. A 3.5 g sample was used for these measurements, sieved to less than 106 μm initial particle size. Activation (five cycles) further reduces the size to approximately 1–4 μm.

2.2. Neutron diffraction

Measurements were made on the powder diffractometer POLARIS at the ISIS pulsed neutron source (Rutherford Appleton Laboratory, UK). The time-of-flight spectra were converted to equivalent fixed-wavelength patterns at $\lambda = 1.32$ Å, as detailed in [4], so that Rietveld analysis could be performed with the same software used for XRD. The sample holder (Fig. 2) is made of thin-walled stainless steel tube, designed for routine operation at up to 1 MPa gas pressure. Large copper heat sinks are fitted to the top and bottom of the cell, cooled and heated by Peltier-effect heat pumps operated by a temperature controller. The pumped heat is supplied or dumped by an external water circuit. The sample temperature is indicated by

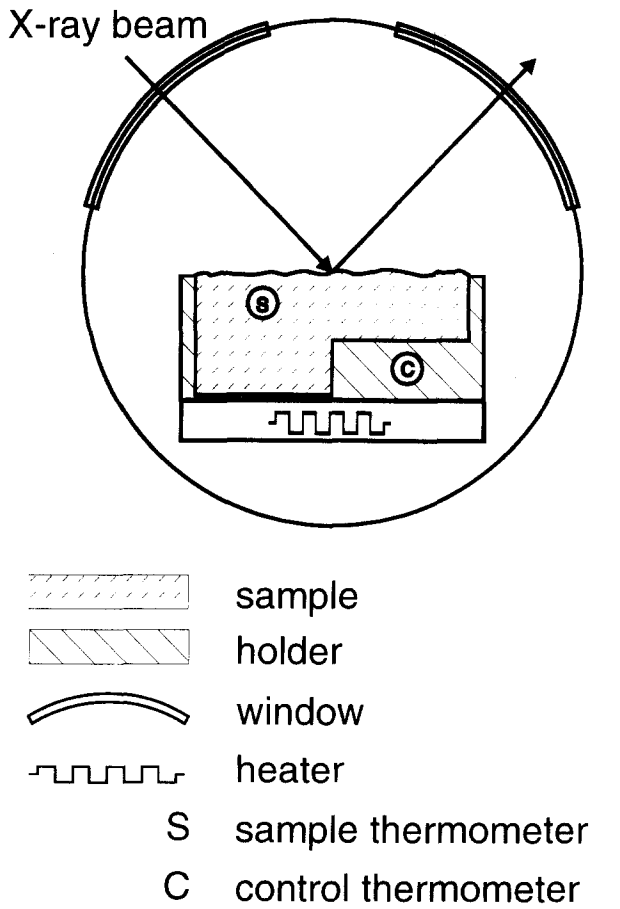

Fig. 1. In situ sample cell used for X-ray powder diffraction; schematic end section.

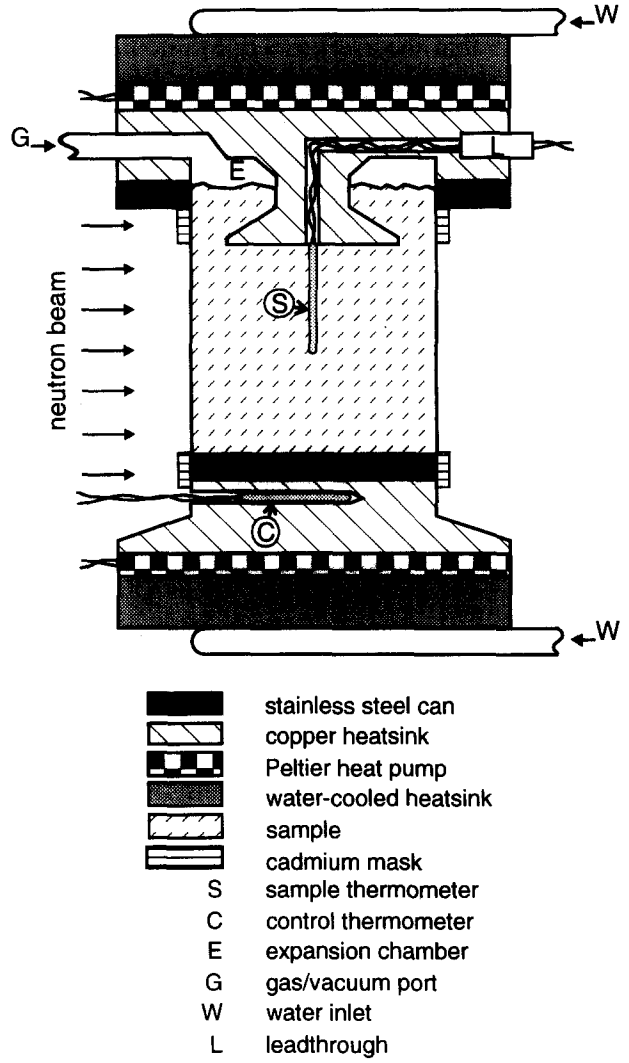

Fig. 2. In situ sample cell used for neutron powder diffraction; schematic side section.

a Pt thermometer buried in the centre of the sample. Operation from about −20 °C to about +50 °C is possible. Near ambient temperature, a temperature stability of ±0.01 °C at the thermometer is achieved over many hours, except during the bursts of enthalpy accompanying absorption and desorption steps. An expansion chamber in the top heat sink keeps the top surface of the powdered sample in contact with the heat sink despite the 24% increase in sample volume between pure $LaNi_5$ and pure β-$LaNi_5$–D.

3. Results

3.1. X-ray diffraction

Fig. 3 shows the evolution with time of the $(101)_\alpha$ and $(101)_\beta$ Bragg peaks while the sample absorbs a large aliquot of H owing to a step change in the hydrogen gas pressure (see Table 1, experiment 2). Despite the

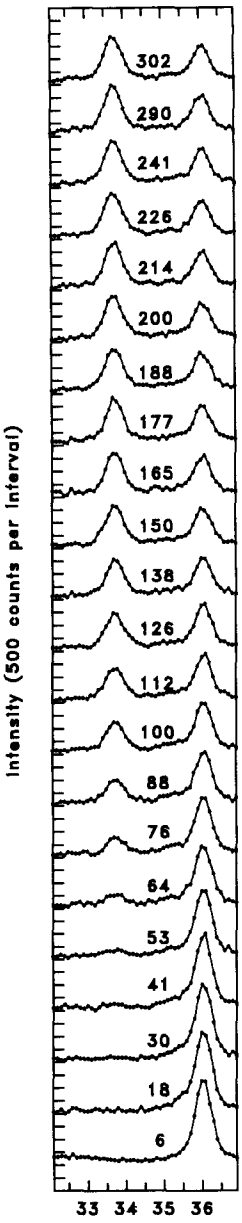

Fig. 3. XRD scans over the $LaNi_5$–H $(101)_\beta$ and $(101)_\alpha$ peaks, at 33.6° and 35.9° 2θ respectively, measured during hydrogen absorption in a single step to [H]/[M] = 0.69 (see Fig. 4). The number on each scan indicates the time in minutes at the centre of the scan. Note the long incubation time (approximately 25 min) and that the conversion of α to β is only half complete after about 100 min.

existence of small amounts of diffuse intensity between the α and β XRD peaks, the transformation is largely discontinuous, i.e. the $(101)_\alpha$ peak does not migrate towards the $(101)_\beta$ position, but is diminished at the same time as the β peak grows. This was confirmed in longer scans (20°–60° 2θ) conducted during the slowest transitions. $\alpha \rightarrow \beta$ conversion in the footprint of the X-ray beam did not begin until more than 20 min after the pressure was applied.

Fig. 4 (bottom) shows the time dependence of the percentage of β phase at the alloy surface, derived from the integrated intensities of the $(101)_\alpha$, diffuse

Table 1
Summary of XRD experiments

Experiment	T (°C)	ΔP (kPa)[a]	ΔT (°C)[b]	$\Delta([H]/[M])$	t_0 (min)[c]
1	20	77	–	0.54	25
2	23	96	9	0.65	41
3	30	10	1	0.13	26
4	30	25	2	0.30	12
5	30	46	5	0.56	6
6	30	55	9	0.68	3–4
7	30	100	8	0.75	21
8	30	190	14	0.85	6
9	30	312	21	0.81	2–3
10	35	310	16	0.81	6
11	20	−108	–	−0.80	43
12	21	−83, −42	−8	−0.54, −0.28	110
13	30	−53, −17	−5	−0.45, −0.20	10
14	35	−40	−9	−0.40	3

[a]Driving pressure, expressed as initial pressure applied to the sample minus the plateau pressure.
[b]Maximum temperature change during absorption or desorption.
[c]Incubation time for the appearance of the β phase, estimated visually from XRD patterns (overestimates relative to JMA equation).

and $(101)_\beta$ diffraction peaks shown in Fig. 3. A Voigt function was fitted to each peak and corrected for the intensity of this peak in the empty alloy compared with the fully hydrided alloy after equilibration for many hours. Owing to fortuitous cancellation of the Lorentz-polarization factor with the effect of lattice expansion, this correction is very close to unity.

Fig. 4 also shows the time evolution of the sample temperature (top) and [H]/[M] (centre) during the same experiment. [H]/[M] rose rapidly from 0.04 to 0.69 (i.e. about 70% of capacity). The sample temperature rose sharply by 9 °C and fell back to the base temperature within 35 min. The slowly rising temperature background in this experiment was due to heat output from the X-ray tube trapped in the shielding box and had no significant influence on these results, as confirmed by later experiments at a controlled base temperature of 30 °C (experiments 3–9 in Table 1). According to the percentage of β phase calculated from [H]/[M] by the lever rule, the phase transformation ceased after about 30 min, whereas the bottom graph shows that at this time the conversion to β phase at the free surface of the sample was in reality just beginning. The onset of the $\alpha \rightarrow \beta$ phase transition at the surface also occurred much later than the temperature excursion at the thermocouple.

Further experiments performed under different conditions of temperature and pressure are summarized in Table 1. The time to the onset of the $\alpha \rightarrow \beta$ ($\beta \rightarrow \alpha$) transition at the sample surface (the incubation time t_0) depends in a complicated way on both the sample temperature and the size of the pressure step used to drive the H transfer. A strong trend appears in ex-

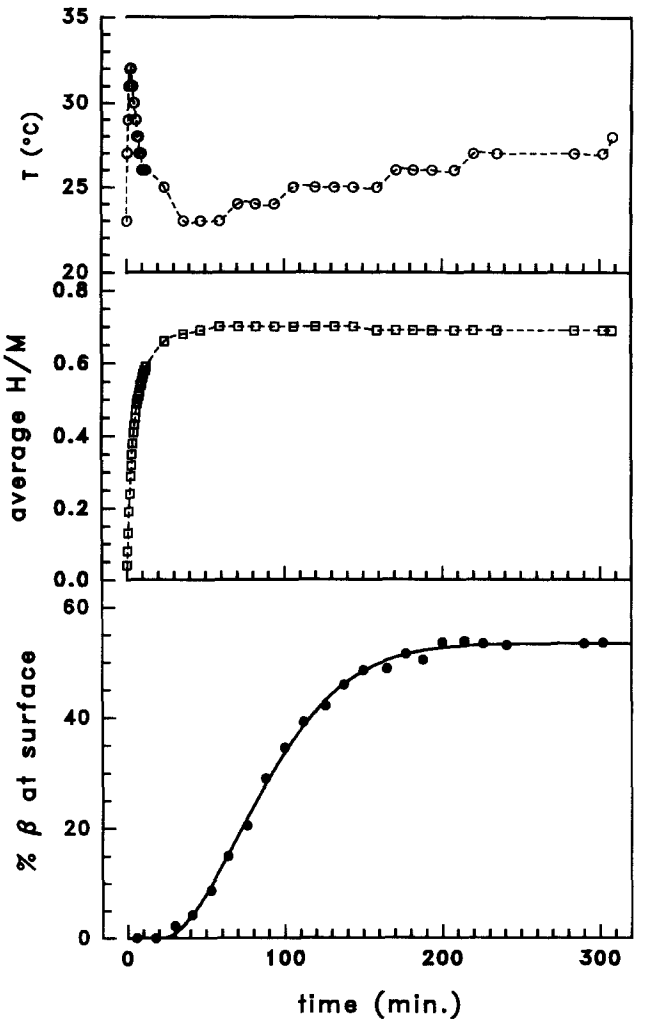

Fig. 4. Absorption of H by $LaNi_5$ to [H]/[M] = 0.69 following a pressure step applied at $t = 0$: top, temperature; centre, hydrogen-to-metal ratio derived from the decrease in H_2 pressure; bottom, percentage of β phase in the footprint of the X-ray beam during hydrogen absorption (●) derived from XRD scans in Fig. 3 using fitted Voigt functions. The solid line is a fit to the Johnson–Mehl–Avrami equation. Note that, whereas T and [H]/[M] begin to change immediately in response to the increase in pressure, phase conversion at the sample surface lags the H absorption by the bulk considerably.

periments 3–6 which were performed consecutively with the pressure drive applied in the same way each time, i.e. from an established position at the start of the absorption plateau. Within this series, increasing ΔP is strongly correlated with increased ΔT and decreased t_0. The same pattern occurs for experiments 7–9, in which ΔP was applied from $P \approx 0$ leading to different values of t_0. Clearly, the detailed way in which the hydrogen pressure is applied to the sample greatly influences the incubation time for β formation at the free surface.

Several experiments (not shown in Table 1) were conducted at 30 °C to determine how much of the absorption plateau of the bulk sample could be traversed

without initiating the $\alpha \rightarrow \beta$ transition at the free surface. By introducing the H_2 aliquot slowly, [H]/[M] = 0.3 could be reached without the β phase appearing at the surface, even after many hours.

3.2. Neutron diffraction

To confirm that the X-ray results are indeed due to macroscopic inhomogeneities, a 13.4 g sample in the neutron sample holder was subjected to a similarly applied rapid absorption to [D]/[M] = 0.65 with the average sample temperature controlled to ±1 °C. Neutron diffraction patterns were recorded at approximately 5 min intervals. The change in percentage of β phase with time during a typical experiment, derived from Rietveld analyses using the neutron data, is plotted in Fig. 5 (closed circles). Given the 300 s averaging time for the ND data, there is a close correspondence with the percentage of β phase calculated from the D_2 pressure interpreted on the standard pressure–composition diagram (method 1 of [4]). This confirms that the X-ray observations apply only to the near-surface region.

The two measurements shown in Fig. 5 begin to disagree at higher [D]/[M]. This is a strong indicator that compositional inhomogeneities occur in the ND sample also. As explained in [4], we believe that the discrepancy arises because β-rich material, formed adjacent to the top heat sink, is pushed up into the expansion chamber (see Fig. 2) and out of the neutron beam. The material in the path of the beam then has a lower than average D concentration.

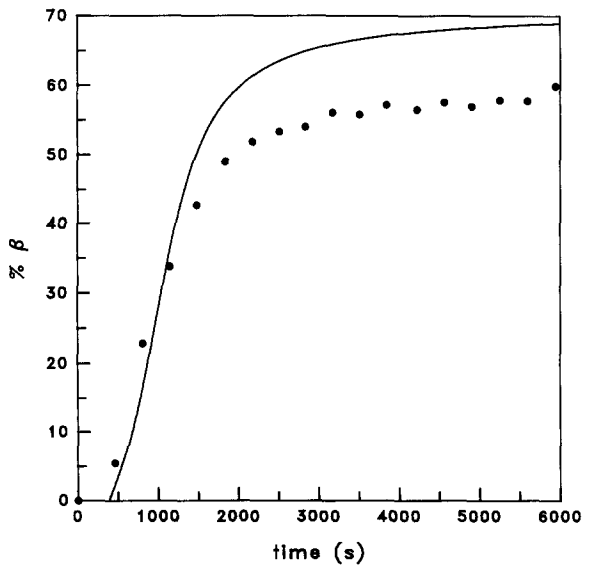

Fig. 5. Measured percentage of β phase (●) from neutron diffraction during D absorption compared with the amount predicted by the pressure–composition phase diagram (—). Note that there is no time delay such as that observed in the X-ray results shown in Fig. 4. The discrepancy at high percentages of β phase is discussed in the text.

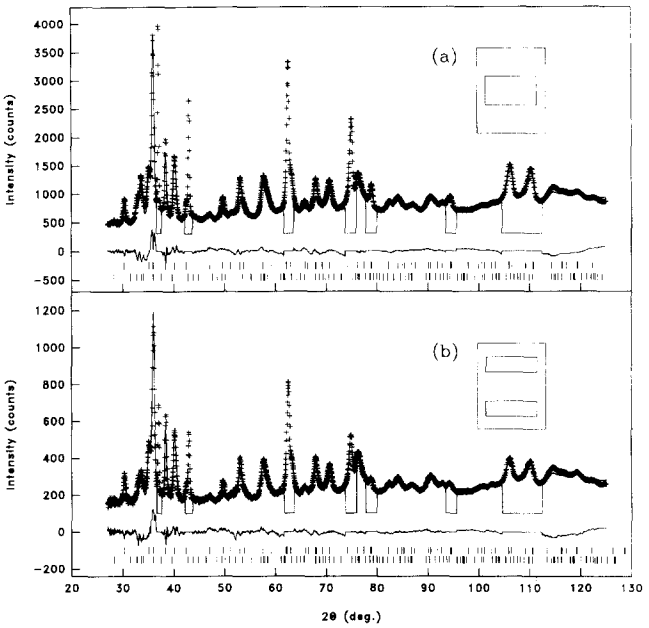

Fig. 6. Rietveld fits to neutron diffraction patterns from sample fractions (a) at the centre of the sample, and (b) adjacent to the heat sinks at the ends of the sample holder. The sample has absorbed to [D]/[M] = 0.30 in a single step. Data are plotted as (+) and the calculated patterns as solid lines. The lower solid lines are difference profiles. The vertical bars below the patterns are reflection markers for the α and β phases respectively. The difference in the amounts of β phase in the two sample fractions is made apparent by inspection of the $(110)_\alpha$ peak near 30° and the $(111)_\beta$ and $(200)_\beta$ peaks near 33°.

In a further experiment designed to verify this conclusion, the sample was taken from [D]/[M] = 0 to [D]/[M] = 0.30 in a single rapid step and allowed to settle for 30 min. The top 25% and bottom 25% of the sample were then masked with Cd to absorb the neutron beam. In this way a pattern was recorded from the centre 50% of the sample. This procedure was repeated with the middle 50% masked while a pattern was recorded from the end portions of the sample, adjacent to the heat sinks. The Rietveld fits to these two patterns are shown in Figs. 6(a) and 6(b) respectively. Scrutiny of the $(110)_\alpha$ peak near 30° and the $(111)_\beta$ and $(200)_\beta$ peaks near 33° shows that the part of the sample nearer the heat sinks has more β phase than the central part. Quantitative phase analysis using the Rietveld scale factors [5] shows that, on average, 17.0% of the sample centre is β phase, whereas an average 26.4% of the end fraction of the sample is β phase.

4. Discussion

The thermal model developed in [1] predicts that a diffuse "reaction front" traverses the sample from heat sink to free surface, with pure α ahead and pure β behind in absorption. The XRD results lend qualitative support to this idea.

The detailed kinetic behaviour of the α–β transformation at the sample surface as revealed by XRD is very complicated, being a convolution of the intrinsic kinetics with the approach of the supposed reaction front from below and the dependence of the X-ray attenuation factor on depth below the surface. The calculated penetration depth for Co Kα radiation in $LaNi_5$ is around 5 μm, so only the topmost exposed particles in the sample contributed to the XRD pattern. For these reasons, no detailed analysis of the actual time behaviour of the phase proportions was attempted. The solid line in the bottom graph of Fig. 4 is a fit by non-linear least-squares regression to the Johnson–Mehl–Avrami (JMA) equation:

$$\%\beta = y_0\{1 - \exp - [k(t - t_0)]^n\}$$

with $k = 0.013$ min^{-1}, $n = 1.73$ and $t_0 = 23$ min. The sigmoidal trend occurs despite the complexity of the kinetics, as previously noted by Bayane et al. [6]. Apart from quantifying the incubation time, however, applying the JMA equation in isolation is not useful.

The behaviour of the incubation time for the appearance of the β phase at the free surface is also in qualitative agreement with the predictions of the model in [1] and its conceptual extension in [2]. In general, higher pressure drive causes faster absorption and an earlier appearance of the β phase at the surface. From the discussion in [2], it is expected that a low pressure drive will increase the effect of temperature gradients on the compositional inhomogeneity; a small increase in local temperature will then be sufficient to raise the local absorption pressure above the available pressure. This appears to be why [H]/[M] = 0.3 could be achieved in the XRD sample without the β phase appearing at the surface; the pressure drive was absorbed before the reaction front could reach the sample surface.

Considered in this light, it can be seen that the substantial spatial inhomogeneity revealed in Fig. 6 was recorded under conditions of high pressure drive, where the effect is in fact minimized by some β phase being quickly formed throughout the sample (see Table 1). Had the aliquot been added to the ND sample very slowly, it is likely that the centre portion would have been free of β phase. Thus it appears that the "reaction front" is sharply defined when moving slowly, and rather diffuse when moving fast.

5. Conclusions

(i) A significant spatial inhomogeneity of the α/β phase proportions in $LaNi_5$–D has been observed.

(ii) Our results support the prediction of [1] that the inhomogeneity arises owing to temperature gradients originating from enthalpy released by the $\alpha \longleftrightarrow \beta$ phase interconversion. Since the data were taken by the isochoral technique, our results are consistent with the conclusion of [2] that it is the falling pressure in an isochoral hydrogenator which facilitates the translation of temperature gradient into compositional inhomogeneity. Further experiments using an isobaric measurement technique are required to prove this point.

(iii) The nature of the X-ray powder diffraction technique means that its use in kinetics studies of metal hydrides is unlikely to give quantitatively meaningful results unless either the thermal design of the sample cell guarantees no thermal gradients, or an isobaric hydrogenation technique is used as suggested in [2].

Acknowledgements

This work was carried out with support from the Energy Research and Development Corporation (project #1429), the Australian Research Council (project A89130053) and the Access to Major Research Facilities Program (Australia). We thank Andrew Chessor for his assistance with the XRD measurements. EMG thanks Dr Pierre Dantzer for helpful discussions and the reprint of Ref. [1]. The assistance of Drs. Ron Smith and Steve Hull at RAL with the ND experiments is gratefully acknowledged.

References

[1] M. Pons and P. Dantzer, *Z. Phys. Chem., 183* (1994) 225.
[2] E.M. Gray, C.E. Buckley and E.H. Kisi, *J. Alloys Comp., 215* (1994) 201.
[3] E.H. Kisi, C.E. Buckley and E.M. Gray, *J. Alloys Comp., 185* (1992) 369.
[4] E.H. Kisi, E.M. Gray and S.J. Kennedy, A neutron diffraction investigation of the $LaNi_5$–D phase diagram, *J. Alloys Comp.*, in press.
[5] R.J. Hill and C.J. Howard, *J. Appl. Crystallogr., 20* (1987) 467–474.
[6] C. Bayane, E. Sciora and N. Gerard, *J. Mater. Sci. Lett., 12* (1993) 1821.